Evolution of strangeness in an equilibrating and expanding quark-gluon plasma

Dipali Pal,* Abhijit Sen, and Munshi Golam Mustafa
Theory Group, Saha Institute of Nuclear Physics, 1/AF Bidhan Nagar, Kolkata 700 064, India

Dinesh Kumar Srivastava
Variable Energy Cyclotron Centre, 1/AF Bidhan Nagar, Kolkata 700 064, India

We evaluate the strangeness production from equilibrating and transversely expanding quark-gluon plasma which may be created in the wake of relativistic heavy-ion collisions. We consider boost-invariant longitudinal and cylindrically symmetric transverse expansion of a gluon-dominated partonic plasma, which is in local thermal equilibrium. Initial conditions obtained from the self-screened parton cascade model are used. We empirically find that the final extent of the partonic equilibration rises almost linearly with the square of the initial energy density. This along with the corresponding variation with the number of participants may help us distinguish between various models of parton production.

I. INTRODUCTION

The study of ultrarelativistic heavy-ion collisions has entered a new era with the successful commissioning of the Relativistic Heavy Ion Collider at Brookhaven. This provides an opportunity to verify the possible occurrence of a phase transition from hadronic matter to deconfined quark matter, where partons are the basic degrees of freedom. At the (lower) SPS energies, an enhanced production of strangeness, considered to be one of the more robust signatures of the quark-hadron phase transition, has already been observed [1–4]. The initial temperatures likely to be attained at RHIC and the LHC are expected to be much larger. A natural question would now be, how quickly is the strangeness equilibrated, if at all?

In heavy-ion collisions strangeness is produced abundantly through the partonic interactions if the temperature $T \geq 200$ MeV, the mass threshold of this semiheavy flavor. The extent of its equilibration would, however, depend upon such details as the thermal and chemical evolution of the partonic system and the lifetime of the hot deconfined phase. It has recently been shown that the chemical equilibration of the light flavors and the gluons slows down due to the radial expansion [5,6]. It should then be expected that the extent of strangeness equilibration can also be affected if allowances are made for the likely radial expansion of the plasma. The present work attempts to get answers to this and related questions. We limit our discussions to the production and evolution of strangeness during the deconfined phase, whose initial conditions are taken from the self-screened parton cascade (SSPC) model [7], which has formed the basis of a large number of related studies in recent times. An early work in this direction used the initial conditions obtained from the HIJING model and considered only a longitudinal expansion [8]. In the following we closely follow this treatment and extend it to include transverse expansion as well.

Our paper has been organized as follows. Section II describes briefly the basic equations of the hydrodynamic and chemical evolution of the partonic gas through the partonic reactions in a $(1+1)$-dimensional longitudinal expansion and a $(3+1)$-dimensional transverse expansion. A brief summary is given in Sec. III.

II. HYDRODYNAMIC EXPANSION AND CHEMICAL EVOLUTION

A. Master equations

We start with the assumption that the early (semi)hard collisions among partons produce a thermalized partonic plasma. The high-p_T partons produced early in the collision then provide a color-screened environment for the production of partons having low p_T and the high density of the partons launches the Landau-Pomeranchuk-Migdal (LPM) suppression mechanism to eliminate the collinear singularity in parton fragmentation. This leads to the the so-called self-screened parton cascade model [7] and can be used to provide plausible initial conditions for the system. The subsequent chemical equilibration is then attained through reactions of the type $gg \leftrightarrow q\bar{q}$ and $gg \leftrightarrow ggg$.

The evolution of the system is now controlled by the equation for conservation of energy and momentum of an ideal fluid:

$$\partial_\mu T^{\mu\nu} = 0, \quad T^{\mu\nu} = (\varepsilon + P)u^\mu u^\nu + P g^{\mu\nu}, \quad (1)$$

where ε is the energy density and P is the pressure measured in the rest frame of the fluid. The four-velocity vector u^μ of the fluid satisfies the constraint $u^2 = -1$.

We assume that the distribution functions for partons can be scaled through equilibrium distributions as

$$f_j(E_j, \lambda_j) = \lambda_j \tilde{f}_j(E_j), \quad (2)$$

     65 034901-1

where $\tilde{f}_j(E_j)=(e^{\beta E_j}\mp 1)^{-1}$ is the Bose-Einstein (BE) [Fermi-Dirac (FD)] distribution for gluons [quarks], and λ_j $(j=g,u,d,s)$ are the nonequilibrium fugacities, $E_j=\sqrt{p_j^2+m_j^2}$, and m_j is the mass of the parton.

Now one can write the number density, energy density, and pressure for a partially equilibrated multicomponent partonic plasma [8]:

$$n=n_g+\sum_i (n_i+n_{\bar{i}})=\left(\lambda_g a_1+\sum_i \lambda_i b_1(x_i)\right)T^3,$$

$$\varepsilon=\varepsilon_g+\sum_i (\varepsilon_i+\varepsilon_{\bar{i}})=\left(\lambda_g a_2+\sum_i \lambda_i b_2(x_i)\right)T^4,$$

$$P=P_g+\sum_i (P_i+P_{\bar{i}})=\frac{1}{3}\left(\lambda_g a_3+\sum_i \lambda_i b_2(x_i)b_3(x_i)\right)T^4,$$

$$(3)$$

where $a_1=16\zeta(3)/\pi^2$ and $a_2=a_3=8\pi^2/15$ and

$$b_1(x_i)=2\frac{d_i}{2\pi^2}\cdot x_i^3\sum_{n=1}^{\infty} (-1)^{n+1}\frac{1}{nx_i}K_2(nx_i),$$

$$b_2(x_i)=2\frac{d_i}{2\pi^2}$$

$$\cdot x_i^4\sum_{n=1}^{\infty} (-1)^{n+1}\left[\frac{3}{(nx_i)^2}K_2(nx_i)+\frac{1}{(nx_i)}K_1(nx_i)\right],$$

$$b_3(x_i)=\frac{\displaystyle\sum_{n=1}^{\infty} (-1)^{n+1}\frac{1}{(nx_i)^2}K_2(nx_i)}{\displaystyle\sum_{n=1}^{\infty} (-1)^{n+1}\left[\frac{1}{(nx_i)^2}K_2(nx_i)+\frac{1}{3}\frac{1}{(nx_i)}K_1(nx_i)\right]},$$

$$(4)$$

for $i=u,d,s$. We also have the color and spin degeneracy $d_i=3\times 2$ and $x_i=m_i/T$, where m_i is the mass of the quark and K's are modified Bessel functions. We take strange quark mass as 150 MeV. For massless quarks these expressions simplify considerably and we have $b_1(0)=2\times 9\zeta(3)/2\pi^2$, $b_2(0)=2\times 7\pi^2/40$, and $b_3(0)=1$. We further assume that $\lambda_i=\lambda_{\bar{i}}$, which should be valid for negligible net-baryonic density. This should be a reasonable approximation at RHIC and LHC energies. The speed of sound (c_s) can be obtained from

$$c_s^2=\frac{dP}{d\varepsilon}.\qquad(5)$$

We found it to be close to $1/\sqrt{3}$, as we confine ourselves to $T\geq 200$ MeV. We must add that several lattice QCD evaluations suggest [9] that $\Delta=\varepsilon-3p\geq 0$ so that $c_s^2<1/3$. For such a situation the cooling of the plasma would be slower [10] and thus a much larger time would be available for equilibration.

We solve the hydrodynamic equations (1) with the assumption that the system undergoes a boost-invariant longitudinal expansion along the z axis and a cylindrically symmetric transverse expansion [11]. It is then sufficient to solve the problem for $z=0$.

The chemical equilibration of the species j is governed by the master equation

$$\partial_\mu(n_j u^\mu)=R_j(x),\qquad(6)$$

where R_j are the rates which propel the system towards chemical equilibration. The system would be in chemical equilibrium when $\lambda_j\equiv 1$ so that $R_j(x)=0$. As mentioned earlier, the dominant chemical reactions through which the chemical equilibration proceed [12] are $gg\leftrightarrow ggg$ and $gg\leftrightarrow i\bar{i}$. Radiative processes involving quarks have substantially smaller cross sections in perturbative QCD, and quarks are less abundant than gluons in the initial phase of the chemical evolution of the parton gas. Other elastic scattering processes ensure maintenance of thermal equilibrium.

Under these assumptions the master equations for different species become [12]

$$\partial_\mu(n_g u^\mu)=(R_{2\to 3}-R_{3\to 2})-\sum_i (R_{g\to i}-R_{i\to g}),$$

$$\partial_\mu(n_i u^\mu)=\partial_\mu(n_{\bar{i}} u^\mu)=R_{g\to i}-R_{i\to g},\qquad(7)$$

in an obvious notation.

The gain and loss term for the gluon fusion process, $gg\leftrightarrow i\bar{i}$ can be written as

$$R_{g\to i}-R_{i\to g}=(\lambda_g^2-\lambda_i\lambda_{\bar{i}})\frac{1}{2}\int \frac{d^3p_1}{(2\pi)^3 2E_1}\int \frac{d^3p_2}{(2\pi)^3 2E_2}$$

$$\times\int \frac{d^3p_3}{(2\pi)^3 2E_3}\int \frac{d^3p_4}{(2\pi)^3 2E_4}\tilde{f}_g(p_1)\tilde{f}_g(p_2)$$

$$\times(2\pi)^4\delta^4(p_1+p_2-p_3-p_4)\sum |\mathcal{M}_{gg\to i\bar{i}}|^2,$$

$$(8)$$

where we have used the unitary relation $|\mathcal{M}_{gg\to i\bar{i}}|^2=|\mathcal{M}_{i\bar{i}\to gg}|^2$. The above integral can be written as free space cross section for fusion process folded with the distributions for initial particles as

$$I_{gg\to i\bar{i}}=\frac{1}{2}\int \frac{d^3p_1}{(2\pi)^3}\int \frac{d^3p_2}{(2\pi)^3}[\sigma_{gg\to i\bar{i}}v_{12}]\tilde{f}_g(p_1)\tilde{f}_g(p_2),$$

$$(9)$$

with the cross section given by

$$d\sigma_{gg\to i\bar{i}} = \frac{1}{v_{12}2E_12E_2} \int \frac{d^3p_3}{(2\pi)^32E_3}$$

$$\times \int \frac{d^3p_4}{(2\pi)^32E_4}(2\pi)^4\delta^4(p_1+p_2-p_3-p_4)$$

$$\times \sum |\mathcal{M}_{gg\to i\bar{i}}|^2, \tag{10}$$

where $v_{12}=|\mathbf{v}_1-\mathbf{v}_2|$, the relative velocity between the initial particles. Following Ref. [12] Eq. (9) can be written

$$I_{gg\to i\bar{i}} = \frac{1}{2}\sigma_2^i\tilde{n}_g^2, \tag{11}$$

so that the rates given in Eq. (8) become

$$R_{g\to i} - R_{i\to g} = \frac{1}{2}\sigma_2^i n_g^2 \left(1-\frac{\lambda_i^2}{\lambda_g^2}\right) = R_2^i n_g \left(1-\frac{\lambda_i^2}{\lambda_g^2}\right). \tag{12}$$

The net rate for the process $gg\leftrightarrow ggg$ can be written as

$$R_{2\to3} - R_{3\to2} = (\lambda_g^2-\lambda_g^3)\frac{1}{2}\int \frac{d^3p_1}{(2\pi)^32E_1}\int \frac{d^3p_2}{(2\pi)^32E_2}$$

$$\times \int \frac{d^3p_3}{(2\pi)^32E_3}\int \frac{d^3p_4}{(2\pi)^32E_4}$$

$$\times \int \frac{d^3p_5}{(2\pi)^32E_5} \sum |\mathcal{M}_{gg\to ggg}|^2 f_g(p_1)$$

$$\times f_g(p_2)(2\pi)^4\delta^4(p_1+p_2-p_3-p_4-p_5). \tag{13}$$

Similarly the integral in Eq. (13) can also be written in factorized form [12]

$$R_{2\to3} - R_{3\to2} = \frac{1}{2}\sigma_3 n_g^2(1-\lambda_g) = R_3 n_g(1-\lambda_g). \tag{14}$$

The density-weighted rates in Eqs. (12),(14) are defined as

$$R_3 = \frac{1}{2}\sigma_3 n_g, \quad R_2^i = \frac{1}{2}\sigma_2^i n_g, \tag{15}$$

where the thermally averaged and velocity-weighted cross sections are

$$\sigma_3 = \langle\sigma_{gg\to ggg}v_{12}\rangle, \quad \sigma_2^i = \langle\sigma_{gg\to i\bar{i}}v_{12}\rangle, \tag{16}$$

where the superscript i in R_2 and σ_2 denotes the fusion process for a given flavor. We give the details of these calculations in the next subsection. In calculating the rates R_2^i and R_3, we have also considered the temperature dependence of the strong coupling constant as

$$\alpha_s(T) = \frac{12\pi}{(33-2\times3)\ln(Q^2/\Lambda_0^2)}, \tag{17}$$

with the cutoff $\Lambda_0=300$ MeV. The scale $Q=2\pi T$ is derived by comparing the inverse of bare gluon propagator in the imaginary time formalism with the static longitudinal propagator [14].

Equation (7) can now be simplified:

$$\frac{1}{n_g}\partial_t(n_g\gamma) + \frac{1}{n_g}\partial_r(n_g\gamma v_r) + \gamma\left(\frac{v_r}{r}+\frac{1}{t}\right)$$

$$= R_3(1-\lambda_g) - 2\sum_i R_2^i\left(1-\frac{\lambda_i^2}{\lambda_g^2}\right),$$

$$\frac{1}{n_i}\partial_t(n_i\gamma) + \frac{1}{n_i}\partial_r(n_i\gamma v_r) + \gamma\left(\frac{v_r}{r}+\frac{1}{t}\right) = R_2^i\frac{n_g}{n_i}\left(1-\frac{\lambda_i^2}{\lambda_g^2}\right),$$
$$\tag{18}$$

where v_r is the transverse velocity and $\gamma=1/\sqrt{1-v_r^2}$.

If we assume the system to undergo a purely longitudinal boost-invariant expansion, Eq. (1) reduces to the well-known relation [15]

$$\frac{d\varepsilon}{d\tau} + \frac{\varepsilon+P}{\tau} = 0, \tag{19}$$

where τ is the proper time. Using Eqs. (3) in Eq. (19), one can obtain the ultrarelativistic equation of motion [8] as

$$\left[\frac{\dot{\lambda}_g}{\lambda_g} + 4\frac{\dot{T}}{T} + \frac{4}{3}\frac{1}{\tau}\right]\varepsilon_g$$

$$+ \sum_i \left[\frac{\dot{\lambda}_i}{\lambda_i} + 4\frac{\dot{T}}{T}\mathcal{D}_\varepsilon(x_i) + \frac{1}{\tau}\left(1+\frac{1}{3}b_3(x_i)\right)\right]\varepsilon_i = 0,$$
$$\tag{20}$$

where

$$\mathcal{D}_\varepsilon(x_i) = \left\{\sum_{n=1}^\infty (-1)^{n+1}\left[\frac{1}{(nx_i)^2}K_2(nx_i) + \frac{5}{12}\frac{1}{(nx_i)}\right.\right.$$

$$\times K_1(nx_i) + \left.\frac{1}{12}K_0(nx_i)\right]\left\}\left\{\sum_{n=1}^\infty (-1)^{n+1}\right.\right.$$

$$\times \left[\frac{1}{(nx_i)^2}K_2(nx_i) + \frac{1}{3}\frac{1}{(nx_i)}K_1(nx_i)\right]\right\}^{-1},$$
$$\tag{21}$$

which reduces to $\mathcal{D}_\varepsilon(0)=b_3(0)=1$ for massless quarks (antiquarks).

Now the master equations (6) can be written as

$$\frac{\dot{\lambda}_g}{\lambda_g} + 3\frac{\dot{T}}{T} + \frac{1}{\tau} = R_3(1-\lambda_g) - 2\sum_i R_2^i\left(1-\frac{\lambda_i^2}{\lambda_g^2}\right) \tag{22}$$

and

$$\frac{\dot{\lambda}_i}{\lambda_i} + 3\frac{\dot{T}}{T}\mathcal{D}_n(x_i) + \frac{1}{\tau} = R_2^i \frac{n_g}{n_i}\left(1 - \frac{\lambda_i^2}{\lambda_g^2}\right), \qquad (23)$$

where

$$\mathcal{D}_n(x_i) = \frac{\displaystyle\sum_{n=1}^{\infty}(-1)^{n+1}\left[\frac{1}{(nx_i)}K_2(nx_i) + \frac{1}{3}K_1(nx_i)\right]}{\displaystyle\sum_{n=1}^{\infty}(-1)^{n+1}\frac{1}{(nx_i)}K_2(nx_i)}, \qquad (24)$$

and $\mathcal{D}_n(0) = 1$, for massless quarks. We can easily see that Eqs. (18) reduce to Eqs. (22),(23) if there is no transverse expansion so that the radial velocity $v_r = 0$. Now one can study evolution of the multicomponent partonic plasma in terms of the parton fugacities by solving the Eq. (23) for longitudinally and Eq. (18) for transversely expanding plasma with the parton chemical equilibration rates.

B. Partons equilibration rates

In this subsection we briefly recall [8,13] the evaluation of equilibration rates for the gluon fusion process ($gg \rightarrow i\bar{i}$) and gluon multiplication process ($gg \rightarrow ggg$).

1. Gluon fusion

The differential cross section given in Eq. (10) can be written as

$$\frac{d\sigma_{gg \rightarrow i\bar{i}}}{dt} = \frac{1}{16\pi\xi(s, m_1^2, m_2^2)}\sum|\mathcal{M}_{gg \rightarrow i\bar{i}}|^2, \qquad (25)$$

where $\xi = s^2 - 2s(m_1^2 + m_2^2) + (m_1^2 - m_2^2)^2$, which reduces to $\xi = s^2$, for massless incident particles. The matrix element for the process $gg \rightarrow i\bar{i}$ can be obtained in terms of Mandelstam variables from Ref. [16] as

$$\sum|\mathcal{M}_{gg \rightarrow i\bar{i}}|^2 = \pi^2 \alpha_s^2\left[\frac{12}{s^2}(M_i^2 - t)(M_i^2 - u)\right.$$

$$+ \frac{8}{3}\frac{(M_i^2 - t)(M_i^2 - u) - 2M_i^2(M_i^2 + t)}{(M_i^2 - t)^2}$$

$$+ \frac{8}{3}\frac{(M_i^2 - t)(M_i^2 - u) - 2M_i^2(M_i^2 + u)}{(M_i^2 - u)^2}$$

$$- 6\frac{(M_i^2 - t)(M_i^2 - u) + M_i^2(u - t)}{s(M_i^2 - t)}$$

$$- 6\frac{(M_i^2 - t)(M_i^2 - u) + M_i^2(t - u)}{s(M_i^2 - u)}$$

$$\left. - \frac{2M_i^2(s - 4M_i^2)}{3(M_i^2 - t)(M_i^2 - u)}\right], \qquad (26)$$

in which M_i is the current quark mass. However, for massless quarks ($q = u$ and d) the above Eq. (26) reduces to

$$\sum|\mathcal{M}_{gg \rightarrow q\bar{q}}|^2 = 16\pi^2\alpha_s^2\left[\frac{3}{4}\frac{ut}{s^2} + \frac{1}{6}\left(\frac{u}{t} + \frac{t}{u}\right) - \frac{3}{8}\right]. \qquad (27)$$

This together with Eq. (25) diverges logarithmically as $u,t \rightarrow 0$. We assume that this logarithmic divergence for massless quarks can be regularized by assigning them mass given by the thermal mass [12]

$$m_{u,d}^2 = \left[\lambda_g + \frac{1}{2}(\lambda_u + \lambda_d)\right]\frac{4\pi}{9}\alpha_s T^2. \qquad (28)$$

For s quarks no such approximation is necessary and we use Eq. (26) with $m_s = 150$ MeV.

Now integrating the matrix element in Eq. (25) over the variable t, between the limits

$$t_{\pm} = M_i^2 - \frac{s}{2}[1 \pm \chi], \qquad (29)$$

one obtains the total cross section

$$\sigma_{gg \rightarrow i\bar{i}}$$

$$= \frac{\pi\alpha_s^2}{3s}\left[\left(1 + \frac{4M_i^2}{s} + \frac{M_i^4}{s^2}\right)\ln\frac{1+\chi}{1-\chi} - \chi\left(\frac{7}{4} + \frac{31}{4}\frac{M_i^2}{s}\right)\right], \qquad (30)$$

where $\chi = \sqrt{1 - 4M_i^2/s}$.

Now the thermally averaged, velocity-weighted cross section is defined as

$$\sigma_2^i = \langle\sigma_{gg \rightarrow i\bar{i}}v_{12}\rangle = \frac{\displaystyle\int d^3p_1 d^3p_2 f_g(p_1)f_g(p_2)\sigma_{gg \rightarrow i\bar{i}}v_{12}}{\displaystyle\int d^3p_1 d^3p_2 f_g(p_1)f_g(p_2)}. \qquad (31)$$

Using $v_{12} = \xi^{1/2}(s,0,0)/2p_1p_2$ and the thermal average of s for a pair of gluons, $\langle s\rangle = 18T^2$, we get

$$\sigma_2^i \approx \frac{9}{4}\left(\frac{\zeta(2)}{\zeta(3)}\right)^2 \sigma_{gg \rightarrow i\bar{i}}|_{M_i, \langle s\rangle = 18T^2}. \qquad (32)$$

Combining Eqs. (15) and (32) we finally obtain the gluon fusion rate.

2. Gluon multiplication

Following Ref. [12] we also estimate the σ_3 for gluon multiplication process from the differential cross section given by [13]

$$\frac{d\sigma_3}{dq_\perp^2 d^2k_\perp dy} = \frac{d\sigma_{el}^{gg}}{dq_\perp^2}\frac{dn_g}{d^2k_\perp dy}\theta\left(\lambda_f - \frac{\cosh y}{k_\perp}\right)$$

$$\times \theta(\sqrt{s} - k_\perp \cosh y), \qquad (33)$$

where the first step function includes the approximate LPM suppression of the induced gluon and the second step function accounts for energy conservation. Here $k_\perp$ denotes the transverse momentum, y is the rapidity of the radiated gluon and $q_\perp$ corresponds the momentum transfer in the elastic collisions. The infrared divergence associated with QCD radiation is regularized by the LPM effect. However, Eq. (33) is still having infrared singularities in both scattering cross sections and radiation amplitudes associated with the gluon propagator. One can, approximately, control all these singularities using the Debye screening mass [13]

$$\mu_D^2 = \frac{6g^2}{\pi^2}\int_0^\infty k f_g(k)dk = 4\pi\alpha_s T^2\lambda_g. \qquad (34)$$

Now the regularized gluon density distribution induced by a single scattering is

$$\frac{dn_g}{d^2k_\perp dy} = \frac{3\alpha_s}{\pi^2}\frac{q_\perp^2}{k_\perp^2[(\mathbf{k}_\perp - \mathbf{q}_\perp)^2 + \mu_D^2]}, \qquad (35)$$

and the regularized small angle gg scattering cross section is

$$\frac{d\sigma_{el}^{gg}}{dq_\perp^2} = \frac{9}{4}\frac{2\pi\alpha_s^2}{(q_\perp^2 + \mu_D^2)^2}. \qquad (36)$$

The mean free path for the elastic scattering is obtained as [13]

$$\lambda_f^{-1} = \frac{9}{8}a_1\alpha_s T\frac{1}{1 + 8\pi\alpha_s\lambda_g/9}. \qquad (37)$$

Integrating the ϕ part analytically we get the gluon multiplication rate as

$$R_3 = \frac{32}{3a_1}\alpha_s T\lambda_g\left(1 + \frac{8}{9}a_1\alpha_s\lambda_g\right)^2\mathcal{I}(\lambda_g), \qquad (38)$$

where

$$\mathcal{I}(\lambda_g) = \int_1^{\sqrt{s}\lambda_f}dx\int_0^{s/4\mu_D^2}dz\frac{z}{(1+z)^2}$$

$$\times\left\{\frac{\cosh^{-1}(\sqrt{x})}{x\sqrt{[x+(1+z)x_D]^2 - 4xzx_D}}\right.$$

$$\left. + \frac{1}{s\lambda_f^2}\frac{\cosh^{-1}(\sqrt{x})}{\sqrt{[1+x(1+z)y_D]^2 - 4xzy_D}}\right\}, \qquad (39)$$

with $x_D = \mu_D^2\lambda_f^2$ and $y_D = \mu_D^2/s$.

In the following subsection we discuss the chemical evolution of different parton species.

TABLE I. Initial conditions for the hydrodynamical expansion phase in central collision of two gold nuclei at BNL RHIC and CERN LHC energies, respectively, from SSPC [7] given in the first and second rows. Initial conditions given in the third and fourth rows are obtained with the same energy densities as before along with $\lambda_u = \lambda_u = \lambda_g = 1$.

Energy	τ_0 (fm/c)	T_0 (GeV)	$\lambda_g^{(0)}$ -	$\lambda_{u(d)}^{(0)}$ -	$\lambda_s^{(0)}$ -	ϵ_0 (GeV/fm^3)
RHIC	0.25	0.67	0.34	0.068	0.034	61.4
LHC	0.25	1.02	0.43	0.086	0.043	425
RHIC	0.25	0.44	1.0	1.0	0.2	61.4
LHC	0.25	0.72	1.0	1.0	0.2	425

C. Evolution of the multicomponent parton plasma

As mentioned earlier we shall be using the initial conditions obtained from the self-screened parton cascade model [7]. Even though they are well known and used in a large number of studies we reproduce them in Table I for the sake of completeness and an easy reference. We have chosen an initial fugacity for the strange quarks as half of that for the light quarks as in Ref. [8]. This is consistent with the assumption, which is often made, that the number of flavors is ≈ 2.5 if the mass of s quark is taken as zero [12]. We show our results for the longitudinal expansion for RHIC (upper panel) and LHC (lower panel) energies in Fig. 1. As the additional parton production consumes energy, the temperature of the partonic plasma drops considerably faster than the ideal Bjorken's scaling $[T = T_0(\tau_0/\tau)^{1/3}$, where T_0 and τ_0, respectively, are initial temperature and time of the parton gas] represented by the dashed line. We see that like the light quarks and gluon, the production of strange quarks continues until late in the evolution. We further note that the extent of equilibration for the strange quarks in comparison to that for the light quarks $(\lambda_s/\lambda_{u,d})$ rises rapidly and once the temperature falls below about 300 MeV ($\sim 2m_s$) it gets more or less frozen by this time. Thus we conclude that the equilibration of strangeness production may imply the existence of quark matter at a temperature of more than about 300 MeV for a time of the order of a few fm/c. The other aspects of variation of $\lambda_g, \lambda_{u,d}$, and T have already been discussed by several authors [5,8,12]. We do note that the plasma is not fully equilibrated chemically at either RHIC or LHC energies by the time the temperature drops below 200 MeV. We do expect that additional quark production may occur due to gluon fragmentations during hadronization [8,17,18] leading to a chemically equilibrated hot hadronic matter.

Before giving our results for transverse expansion we need to specify the profile of the initial energy density and the fugacity of the partonic system. Following Refs. [6,19,20] we take the initial energy density as

$$\varepsilon(r, \tau_0) = \frac{3}{2}\varepsilon_0\left[1 - \frac{r^2}{R^2}\right]^{1/2}\Theta(R - r), \qquad (40)$$

where R is the transverse dimension of the system, r is the radial distance, and ε_0 is the "average" initial energy density
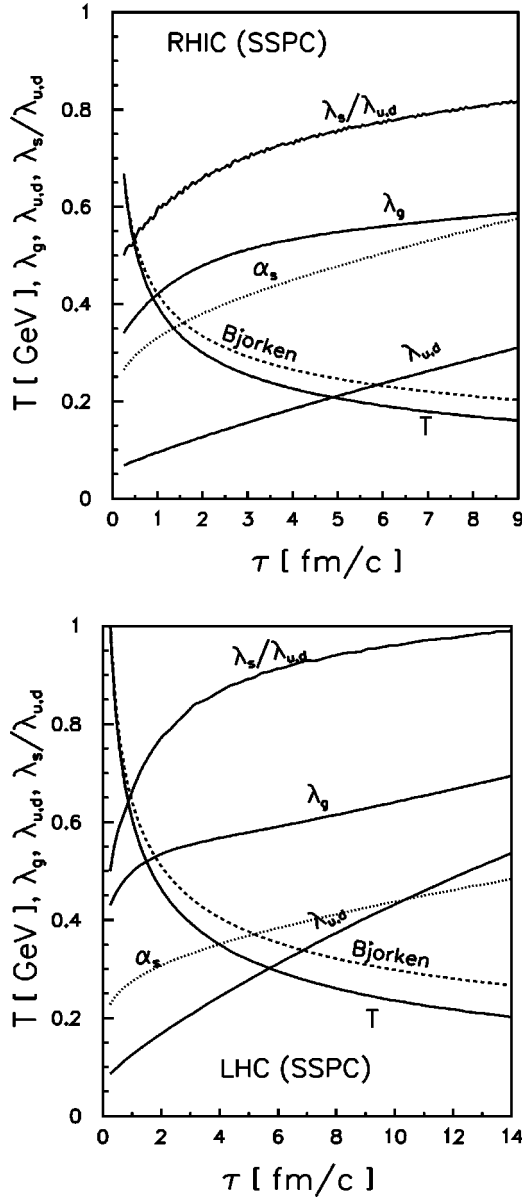
FIG. 1. Variation of temperature, coupling constant, and gluon and quark fugacities with proper time for $(1+1)$-dimensional hydrodynamic expansion with SSPC initial conditions for RHIC (upper panel) and LHC (lower panel) energies.

(see Table I). The profile plays an important role in defining the boundary of the hot and dense deconfined matter and affects the transverse expansion through the introduction of pressure gradients. We have further taken $\lambda_j(r,\tau_0) \propto \varepsilon(r,\tau_0)$ as before [6,19,20]. Any other variation will require an additional parameter. We give our results for the radial variation of λ_g, $\lambda_{u,d}$, and $\lambda_s/\lambda_{u,d}$ in Figs. 2 and 3 for RHIC and LHC energies, respectively, for various times along the constant energy density contours with $\tau = N\tau_0$. Here N is defined [5,19] through $\varepsilon(r,\tau) = \varepsilon(r=0,\tau_0)/N^{4/3}$.

We see that the fugacities attain their highest values near $r=0$ and rise rapidly first and only slowly later in time. We also see a result unique to chemical evolution with transverse expansion that the fugacities may even start reducing to-
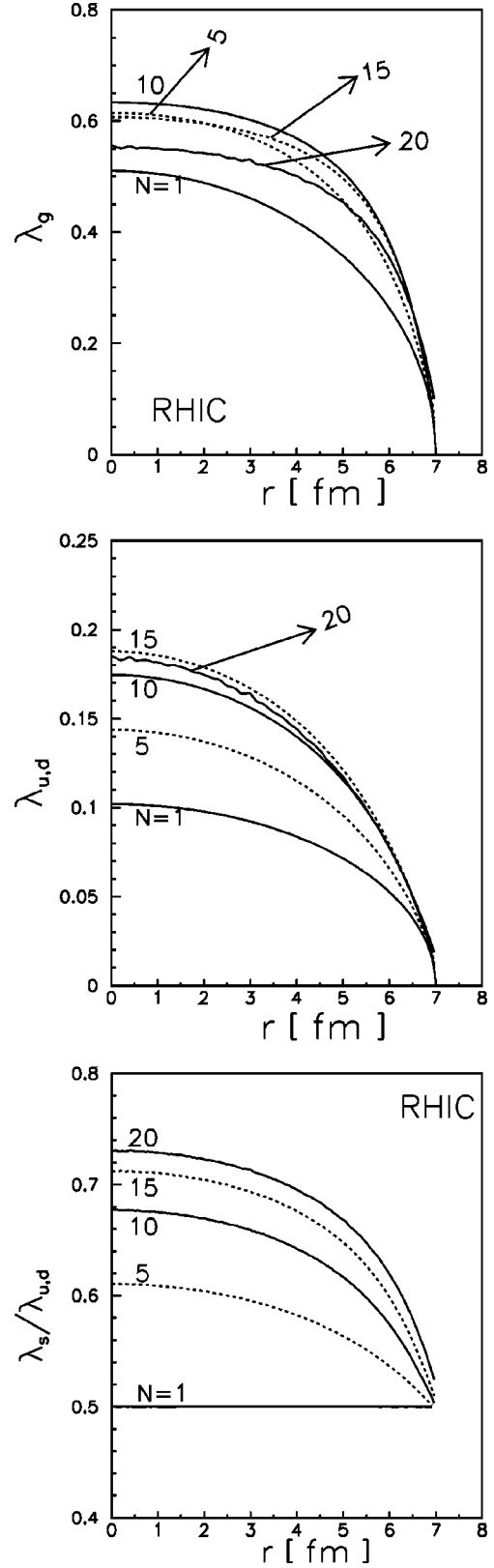

FIG. 2. Variation of gluon (upper panel), massless quark (middle panel) fugacities, and ratio of strange to nonstrange quark fugacity (lower panel) with the transverse radius for RHIC energy at different times $\tau = N\tau_0$, along the constant energy density contours defined by $\varepsilon(r,\tau) = \varepsilon(r=0,\tau_0)/N^{4/3}$.
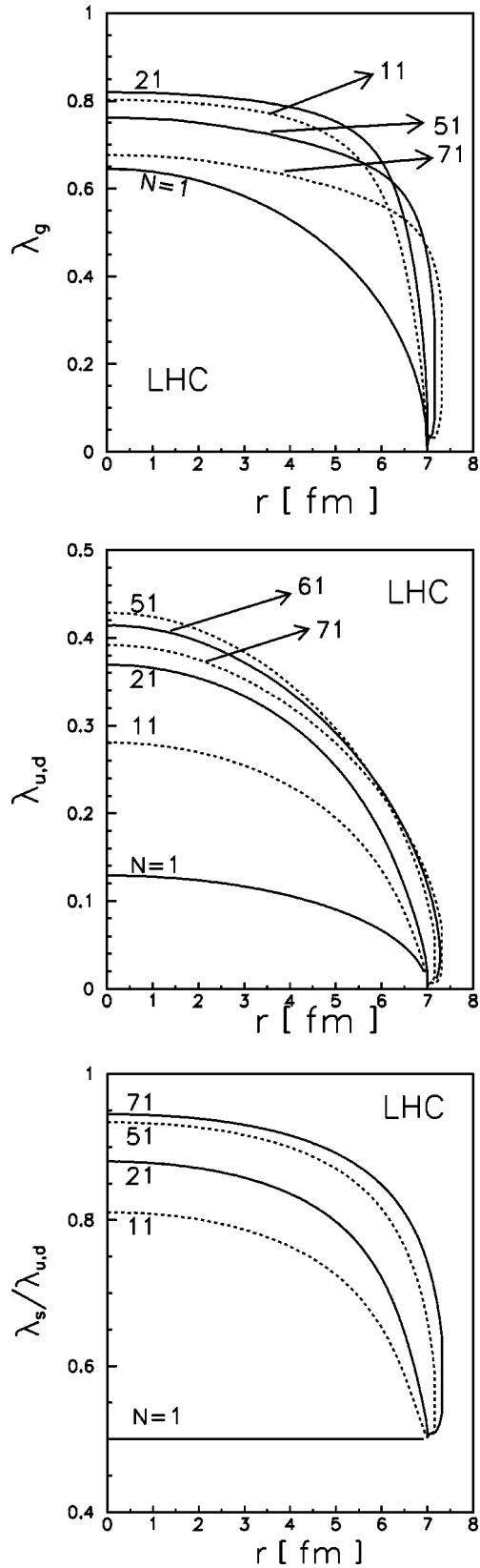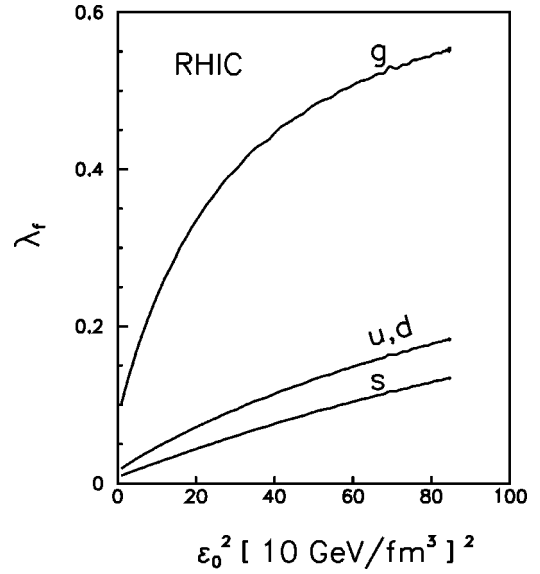
FIG. 4. Variation of the final fugacities with the initial energy density for RHIC energy. Note the scale of the x axis.

We can use our results for the radial variation of the energy density and the fugacities obtained here to estimate the extent of partonic equilibration as a function of the initial energy density. Comparing results for this from Figs. 4 and 5 we note that once the energy density is beyond about $20-40$ GeV, the final fugacities for all the partons increase almost linearly with the square of the energy density. This is a very interesting result.

Let us identify the "local" energy density at the radius r with the average energy density attained in a noncentral collision or with a central collision involving lighter nuclei. Recall that the partonic models suggest that the initial temperature attained in such collisions through the production of minijets varies as $A^{1/6}$ [21,22]. This should then imply that the extent of equilibration of strangeness produced would
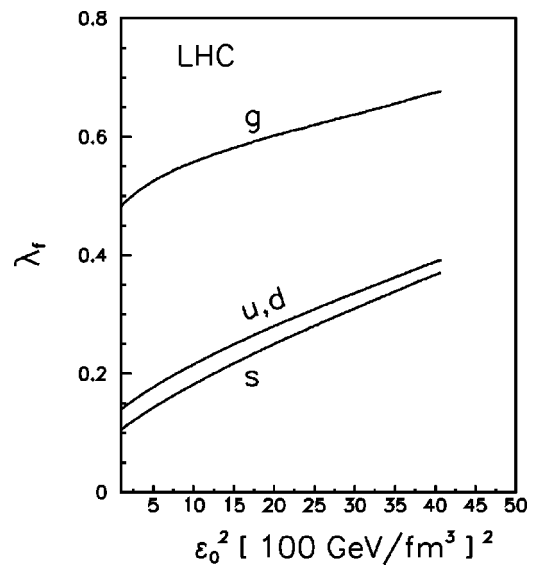

FIG. 3. Same as Fig. 2 for LHC energy.

ward the end of the QGP phase when the radial velocity (gradient) becomes very large (see Ref. [5] for an explanation).

FIG. 5. Same as Fig. 4 for LHC energy. Note the scale of the x axis.

rise as $N_{part}^{4/3}$, if we can identify A with $N_{part}/2$, where N_{part} is the number of participants. In actual cases the variation may be somewhat modified from this naive expectation due to the considerations of shadowing and jet quenching [23].

If on the other hand the energy densities, etc., are decided by the considerations of parton saturation [24], then the initial temperature would vary as $\sim A^{0.126}$ and the energy density as $\sim A^{0.5}$. The results of Figs. 4 and 5 would then imply that the extent of strangeness equilibration should increase as the number of participants, N_{part} (see also Ref. [25] for a slight reformulation of the parton saturation model).

It is also interesting to note that a recent analysis [26] of the centrality dependence of the extent of strangeness equilibration at CERN SPS energies in Pb+Pb collisions gives a linear increase for this with the number of participants.

D. Comparison with other works

Rafelski and Letessier have studied the strangeness equilibration for more than two decades in various details. We shall refer to only a recent work by these authors [27]. In Ref. [27] the following assumptions have been made which are at variance with our works.

(i) The light quarks and gluons are assumed to have attained chemical equilibrium ($\lambda_g = \lambda_u = \lambda_d = 1$) when the evolution of strangeness begins.

(ii) A Boltzmann approximation is used to describe the phase space distribution of s quarks.

(iii) The flavor changing process $q\bar{q} \leftrightarrow s\bar{s}$ has been included. We have neglected them assuming that the gluon fusion process $gg \leftrightarrow s\bar{s}$ dominates in a chemically undersaturated plasma.

Now in the Boltzmann limit the evolution of the s-quark fugacity can be written from Eq. (23) as

$$\frac{\dot{\lambda}_s}{\lambda_s} + 3\frac{\dot{T}}{T}\left[1 + \frac{x_s}{3}\frac{K_1(x_s)}{K_2(x_s)}\right] + \frac{1}{\tau} = R_2^s\frac{n_g}{n_s}\left(1 - \frac{\lambda_s^2}{\lambda_g^2}\right). \quad (41)$$

This can be rewritten as

$$\dot{T}\tilde{n}_s\left[\frac{d\lambda_s}{dT} + \frac{\lambda_s}{T}x_s\frac{K_1(x_s)}{K_2(x_s)} + 3\frac{\lambda_s}{T}\right] + \frac{n_s}{\tau} = R_2^s n_g\left(1 - \frac{\lambda_s^2}{\lambda_g^2}\right), \quad (42)$$

which corresponds to Eq. (11) of Ref. [27]. We see that the third and fourth terms on the left-hand side here are absent in Eq. (11) of Ref. [27], due to the above discussion. One can thus see that the extent of strangeness equilibration attained in the work of Ref. [27] is much larger than in the present work.

As a further check, we have repeated our calculations, assuming $\lambda_g = \lambda_u = \lambda_d = 1$ with the same energy density as before (see Table I) and further taking $\lambda_s(\tau_0) = 0.2$ as in the work of Ref. [27]. We found that now our parameter λ_s rises to about 0.4 at RHIC energies and up to 0.72 at LHC energies, for the case of longitudinal expansion (see Fig. 6). When the transverse expansion is allowed these numbers reduce to 0.66 at LHC energies and 0.38 at RHIC energies,
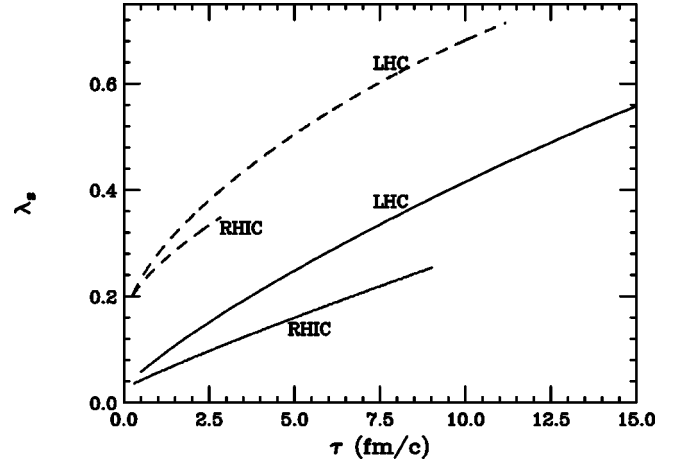

FIG. 6. Sensitivity of the strangeness equilibration to the initial conditions for longitudinal expansion. The solid curves give the results corresponding to Fig. 1 given earlier, while the dashed curves correspond to initial conditions which have the same energy densities as before, but have $\lambda_u = \lambda_u = \lambda_g = 1$ and $\lambda_s = 0.2$, as given in Table I.

respectively. We thus realize that the extent of equilibration of strangeness depends sensitively on the initial conditions and also on the evolution mechanism.

Wong has studied [28] the chemical equilibration of plasma essentially in a formalism similar to that used in the present work, but only with longitudinal expansions. His values for α_s are also much larger.

III. SUMMARY

We have studied the evolution and production of strangeness through the partonic interactions in a chemically equilibrating and expanding multicomponent partonic gas with the initial conditions obtained from SSPC model. We find that most of the strange quarks are produced when the temperature is still more than about 300 MeV ($\sim 2m_s$). Thus a chemically equilibrated plasma is expected to imply the existence of QGP phase for a duration of several fm/c. We also find approximately that the extent of strangeness equilibration rises linearly with the square of the initial energy density within our approach. This may help us to obtain the scaling of the initial energy density with the number of participants and distinguish between the minijet and the partonic saturation models of parton production. It is rather interesting that the charged particle multiplicity in Au+Au collisions at $\sqrt{s_{NN}} = 130$ GeV measured by the PHENIX Collaboration [29] shows a behavior which is a superposition of two terms, a linear increase with the number of participants and a linear increase with the number of collisions (which varies as $N_{part}^{4/3}$).

ACKNOWLEDGMENTS

[1] J. Rafelski, Phys. Rep. **88**, 331 (1982); P. Koch, B. Müller, and L. Rafelski, *ibid.* **142**, 167 (1986); M. Gyulassy, Nucl. Phys. **A418**, 594c (1984).

[2] T. Matsui, B. Svetitsky, and L. D. McLerran, Phys. Rev. D **34**, 783 (1986); **34**, 2047 (1986).

[3] K. Geiger, Phys. Rev. D **48**, 4129 (1993).

[4] J. Letessier and J. Rafelski, Nucl. Phys. **A661**, 497c (2000); Phys. Rev. C **59**, 947 (1999); J. Phys. G **25**, 295 (1999).

[5] D. K. Srivastava, M. G. Mustafa, and B. Müller, Phys. Lett. B **396**, 45 (1997); Phys. Rev. C **56**, 1064 (1997).

[6] D. M. Elliott and D. H. Rischke, Nucl. Phys. **A671**, 583 (2000).

[7] K. J. Eskola, B. Müller, and X. N. Wang, Phys. Lett. B **374**, 20 (1996).

[8] P. Levai and X.-N. Wang, hep-ph/9504214.

[9] E. Laermann, Nucl. Phys. **A610**, 1c (1996).

[10] D. Pal, B. K. Patra, and D. K. Srivastava, Eur. Phys. J. C **17**, 179 (2000).

[11] H. von Gersdorff, L. McLerran, M. Kataja, and P. V. Ruuskanen, Phys. Rev. D **34**, 794 (1986).

[12] T. S. Biro, E. van Doorn, B. Müller, M. H. Thoma, and X. N. Wang, Phys. Rev. C **48**, 1275 (1993).

[13] P. Levai, B. Müller, and X.-N. Wang, Phys. Rev. C **51**, 3326 (1995).

[14] See, e.g., M. H. Thoma, in *Application of High Temperature Field Theory, Quark-Gluon Plasma 2*, edited by R. C. Hwa (World Scientific, Singapore, 1995), p. 51.

[15] J. D. Bjorken, Phys. Rev. D **27**, 140 (1983).

[16] B. L. Combridge, Nucl. Phys. **B151**, 429 (1979).

[17] R. Stock, Phys. Lett. B **456**, 277 (1999).

[18] J. Ellis and K. Geiger, Phys. Rev. D **54**, 1967 (1996).

[19] B. Müller, M. G. Mustafa, and D. K. Srivastava, Heavy Ion Phys. **5**, 394 (1997).

[20] B. K. Patra and D. K. Srivastava, Phys. Lett. B **505**, 113 (2001).

[21] R. C. Hwa and K. Kajantie, Phys. Rev. Lett. **56**, 696 (1986).

[22] X.-N. Wang, Phys. Rep. **280**, 287 (1997).

[23] X.-N. Wang and M. Gyulassy, Phys. Rev. Lett. **86**, 3496 (2001).

[24] K. Eskola, K. Kajantie, P. V. Ruuskanen, and K. Touminen, Nucl. Phys. **B570**, 379 (2000).

[25] D. Kharzeev and M. Nardi, Phys. Lett. B **507**, 121 (2001).

[26] J. Cleymans, B. Kaempfer, and S. Wheaton, nucl-th/0110035.

[27] J. Rafelski and J. Letessier, Phys. Lett. B **469**, 12 (1999).

[28] S. M. H. Wong, Phys. Rev. C **58**, 2358 (1998); **56**, 1075 (1997).

[29] PHENIX Collaboration, K. Adcox *et al.*, Phys. Rev. Lett. **86**, 3500 (2001).